

DEEP OPTICAL IMAGES OF MALIN 1 REVEAL NEW FEATURES

GASPAR GALAZ¹, CARLOS MILOVIC^{2,3,4}, VINCENT SUC^{1,5}, LUIS BUSTA⁶, GUADALUPE LIZANA¹, LEOPOLDO INFANTE^{1,7},
SANTIAGO ROYO⁵*Draft version March 3, 2024*

ABSTRACT

We present Megacam deep optical images (g and r) of Malin 1 obtained with the 6.5m Magellan/Clay telescope, detecting structures down to ~ 28 B mag arcsec⁻². In order to enhance galaxy features buried in the noise, we use a noise reduction filter based on the total generalized variation regularizator. This method allows us to detect and resolve very faint morphological features, including spiral arms, with a high visual contrast. For the first time, we can appreciate an optical image of Malin 1 and its morphology in full view. The images provide unprecedented detail, compared to those obtained in the past with photographic plates and CCD, including HST imaging. We detect two peculiar features in the disk/spiral arms. The analysis suggests that the first one is possibly a background galaxy, and the second is an apparent stream without a clear nature, but could be related to the claimed past interaction between Malin 1 and the galaxy SDSSJ123708.91 + 142253.2. Malin 1 exhibits features suggesting the presence of stellar associations, and clumps of molecular gas, not seen before with such a clarity. Using these images, we obtain a diameter for Malin 1 of 160 kpc, ~ 50 kpc larger than previous estimates. A simple analysis shows that the observed spiral arms reach very low luminosity and mass surface densities, to levels much lower than the corresponding values for the Milky Way.

Subject headings: galaxies: general — galaxies: spiral — techniques: image processing

1. INTRODUCTION

One of the main factors precluding the observability of the extragalactic universe is the limitation in surface brightness (SB) by different surveys. In the seventies, different authors have shown that the universe is populated by low surface brightness galaxies (LSBGs) having much lower SB than the dark night sky (Disney 1976; Bothun et al. 1987). Dalcanton et al. (1997) showed using data from CCD drift scans from the eighties, that one can expect about 4 galaxies/deg² between the range 23-25 mag arcsec⁻². In the nineties and already entering in the new millennium, there were no surveys with significantly fainter surface brightness limits. Some progress on the statistical significance of the population of LSBGs has been made in recent years because of the higher volumes sampled, thanks to massive surveys like the SDSS and others, but still barely reaching ~ 23.0 mag arcsec⁻². On the other hand, and quite unexpectedly, van Dokkum et al. (2015); Koda et al. (2015) reported on the discovery of a dozen of Milky Way (MW) sized, passively evolving, ultra diffuse galaxies (UDG) in the Coma cluster. This population is very likely

dark-matter dominated and thus represents a challenge to the current theories of galaxy formation. Without the presence of large fractions of dark matter in LSBGs, it is very difficult to prevent the rapid destruction of low density galaxies within a massive cluster like Coma (Toomre & Toomre 1972; Moore et al. 1999; McGee & Balogh 2010).

Thus, there are still many unsolved issues concerning the nature of LSBGs. One of these issues is the nature of the class of the so-called giant LSBGs: large format spiral galaxies with a similar or larger size than the MW and very low SB. Big spirals exhibiting similar morphologies of the grand design spiral galaxies like M31 and the MW, but with much lower stellar density, as described in Sprayberry et al. (1995); Impey et al. (1996); Galaz et al. (2002, 2011), and references therein. The best and more extreme example in this category is Malin 1, a disk/spiral active galaxy (Impey & Bothun 1989; Barth 2007) with a disk SB of ≥ 24 B mag arcsec⁻², an uncertain inclination (the HI data indicate that this galaxy has an inclination of about 50 deg), and a barred inner disk (Barth 2007). In addition to this faint SB, what makes Malin 1 exceptional is its size: about 110 kpc diameter in HI and presumably a similar or larger diameter in the optical, making this galaxy the largest one in the universe detected so far (~ 6.5 times the MW diameter). Malin 1 was serendipitously discovered by Bothun et al. (1987) in photographic plates. It is close to NGC 7145 in the Virgo cluster, and near a bright star. This last feature prevents to obtain deep optical imaging easily without contaminating the FOV with scattered light, imposing additional difficulties for observing its morphology. Malin 1 has been studied so far in HI (Pickering et al. 1997; Lelli et al. 2010), and in the optical (Barth 2007; Moore & Parker 2006). It is from these studies that its huge size was measured. Also,

¹ This paper includes data gathered with the 6.5 meter Magellan Telescopes located at Las Campanas Observatory, Chile.

² Instituto de Astrofísica, Pontificia Universidad Católica de Chile.

³ Departamento de Ingeniería Eléctrica, Pontificia Universidad Católica de Chile.

⁴ Centro de Imágenes Biomédicas, Pontificia Universidad Católica de Chile.

⁵ PixInsight Development Team, Pleiades Astrophoto S.L., Spain.

⁶ Centre for the Development of Sensors, Instruments and Systems, UPC-BarcelonaTech.

⁷ Institute for Astro and Particle Physics, Universitat Innsbruck.

⁸ Centro de Astro-Ingeniería, Pontificia Universidad Católica de Chile.

the HI data allow to estimate a HI mass of $\sim 10^{10} M_{\odot}$, and a dynamical mass of $\sim 10^{12} M_{\odot}$, which makes Malin 1 to be an enormous dark matter reservoir (Seigar 2008). The galaxy has been also an interesting target for Spitzer (Rahman et al. 2007) and for sub-mm observations (Das et al. 2006), both for searching warm and cold dust, as well as to detect emission from molecular clouds. These observational efforts failed subsequently, which means that Malin 1 has a very low gas density and/or low dust content. These observational facts place Malin 1 at the bottom end of the Krumholz diagram (Krumholz & McKee 2005), which relates the stellar formation efficiency and the gas surface density. In this diagram Malin 1 is certainly one of the galaxies having the lowest stellar formation efficiency with one of the lowest molecular gas density.

In spite of the wealth of information for Malin 1, including HST imaging (O’Neil et al. 2000) and ground-based observations (Moore & Parker 2006; Reshetnikov et al. 2010), optical images usually lack of good quality and are not deep enough to detect features fainter than $24 B \text{ mag arcsec}^{-2}$. For example, HST observations of Malin 1 (O’Neil et al. 2000) are about 15 minutes exposure, reaching data basically for the bulge of the galaxy, but extremely shallow images for other structures, including the disk and the presumed spiral arms. Moore & Parker (2006) built deep imaging of Malin 1 co-adding R images from 63 UKST photographic films digitally scanned by the superCOSMOS machine, covering the astonishing area of 36 deg^2 . Reshetnikov et al. (2010) obtained spectroscopic observations for the central part of Malin 1 to prove that Malin 1B, a galaxy located 14 kpc from the Malin 1 center, is interacting with Malin 1. But they do not provide optical imaging. Also relevant for this discussion is the work by Barth (2007), which claim that Malin 1 is a normal galaxy (with a normal disk), embedded into a larger, more diffuse very low SB disk. However, in his analysis, Barth uses the same O’Neil et al. (2000) HST images, which are relatively shallow ones. In summary, no deep, high quality CCD images are available for Malin 1.

In this letter we present deep optical images taken with Megacam at the 6.5m Magellan/Clay telescope. We exposed for about 4.5 hours in r and g , reaching $\sim 28 B \text{ mag arcsec}^{-2}$, which allows to observe for the first time features with unprecedented detail. We perform a careful reduction and we use a novel image processing in order to enhance data practically buried into the noise.

The paper is organized as follow. In §2 we present the observations and key steps in the data reduction, in §3 the main results and discussion. We conclude in §4. Through this paper we use $H_0 = 71 \text{ km s}^{-1} \text{ Mpc}^{-1}$; $\Omega_M = 0.27$; $\Omega_{\Lambda} = 0.73$.

2. OBSERVATIONS AND DATA REDUCTION

Observations were performed at the 6.5m Magellan/Clay telescope using Megacam with filters r and g , on the night of 25 April 2014. The night was dark, moonless, a necessary restriction for low SB targets. The night was also photometric with a median seeing of 0.8 arcsec. Exposure times were 4.8 hrs in r and 4.2 hrs in g (individual images of 10 minutes). After cosmic rays rejection, individual images were flat-field and illumination corrected, then stacked, and properly combined (see left

panels of Figure 1). The flat-field and illumination corrections are critical steps. Pixel to pixel variations along the images, as well as illumination inhomogeneities both can introduce mid- and large scale image artifacts that can be erroneously attributed to physical features of the target. In addition to the low SB of Malin 1, the field where the galaxy is located makes difficult to obtain deep images. First, a bright star of 8.5 mag (BD+15 2483) is located 4.7 arcmin SW of Malin 1. Second, the galaxy NGC4571 is located 6.6 south of Malin 1. These two sources generate scattered light and sky brightness which contaminate the already faint structure of Malin 1. To combine different frames, synthetic background models were extracted. These models allow to remove large scale components preventing a proper match between frames. Frame matching, image registration, image combination, and all further post-processing steps were done using Pix-Insight, co-developed by one of the authors of this letter (Conejero, Milovic & Peris 2015). The average sky SB was $20.2 r \text{ mag arcsec}^{-2}$, and $21.8 g \text{ mag arcsec}^{-2}$, equivalent to $\sim 22.5 B \text{ mag arcsec}^{-2}$, using the filter transformations from Jordi, Grebel & Ammon (2006).

2.1. Noise treatment and Multiscale Processing

Given the extremely low SB nature of Malin 1 disk/spiral arms, after the basic image processing described before (calibration and image combining), we perform a more sophisticated procedure in order to enhance the signal. For this task we applied a noise reduction filter based on the *total generalized variation regularizator* (Bredies 2010), TGV hereafter. This is similar to an anisotropic diffusion filter, promoting piecewise smooth images instead of piecewise constant images as is common with these filters. This denoising filter was applied to both r and g images. These were then integrated into a false color image, assigning r data to the red channel, g data to the blue channel, and using a weighted average to create a synthetic green channel. Later, the images were de-linearized, by applying a histogram transform which uses the rational interpolation mid-tones transfer function described by Schlick (1994). This provides more contrast to low signal features than a standard gamma transform. To enhance and isolate the structures of large diffuse objects, pinpoint sources (i.e. stars) were removed from the images using an inpainting algorithm based on TGV. This separation between features is needed, because stars are very contrasted objects, and their signal dominates in the wavelet domain. Direct filtering leads to Gibbs or ringing artifacts, or could enhance structures that correspond to regions of different stellar density, instead of enhancing the smooth background signal. Once those features are isolated, local contrast is enhanced using the starlet transform (also known as *à trous Wavelets*) (Stark 2010). Basically, the image is decomposed into layers with a redundant decomposition, isolating structures at certain characteristic sizes. Wavelet coefficients are modified with multiplicative factors to enhance features at each layer. Finally, small and large scale objects were combined again to achieve the images presented in right panels of Figure 1. All the processing steps were performed on a per-channel basis, and no information was transferred through them. To allow a better visual inspection of the image, an inverted and monochrome version is also presented (bot-

tom panels of Figure 1, and Figures 2 and 3).

2.2. Photometric calibrations and surface brightness

In order to assess our SB limit, it is necessary to photometrically calibrate the images. We have observed Landolt standards, and used the photcal package within IRAF to obtain the photometric solutions. Then, and knowing the pixel size ($0.16 \text{ arcsec pix}^{-1}$), we estimate that the SB we reach in our flat-corrected and combined images at 4σ is $\sim 26.5 \text{ mag arcsec}^{-2}$ in the r band and $\sim 27.5 \text{ mag arcsec}^{-2}$ in the g band, as observed in regions R3 and R6 labeled in Figure 3. These values translate to $\sim 28 \text{ } B \text{ mag arcsec}^{-2}$. This is $\sim 3 - 4 \text{ mag arcsec}^{-2}$ fainter than the typical SB reached by surveys and other works to date (Moore & Parker 2006).

3. RESULTS AND DISCUSSION

Figure 1 shows several panels where Malin 1 is presented. Left panels represent the stacked and combined images. Right panels show the images with the additional TGV treatment. In the top panels, the combined RGB images of the field are presented (see §2.1). In the bottom panels, the inverted and monochrome version of the same image is shown. Some morphological features are clearly seen, especially in the right panels. Some of them observed for the first time.

3.1. Bulge, spiral arms and stellar density

Figure 1 shows clear images of a face-on spiral galaxy presenting a bright inner region which reproduces the image from Barth (2007). In Figure 2 we compare with the HST/WFPC2 image from Barth (2007). The inner region of Malin 1 appears much redder than any other structure visible in the galaxy. Figures 1 and 2 show that Malin 1 exhibits well formed spiral arms. This demonstrates that in ultra-faint disk LSBGs the spiral structure can be well developed to very faint surface brightness limits. In order to quantify the density contrast of the spiral arms, we can compare the estimated density of these structures with the stellar density in the solar neighborhood. The MW disk at the solar vicinity has a stellar mass surface density of $\sim 49 \text{ } M_{\odot} \text{ pc}^{-2}$ (Flynn et al. 2006). From the same author, the luminosity surface density is $25.6 \text{ } L_{\odot} \text{ pc}^{-2}$, or $23.5 \text{ mag arcsec}^{-2}$ in the B band. Converting the observed SB of $\sim 28 \text{ } B \text{ mag arcsec}^{-2}$ in luminosity surface density in solar units, we obtain $\sim 0.41 \text{ } L_{\odot} \text{ pc}^{-2}$, i.e. about 62 times lower than the surface luminosity density in the solar neighborhood indicated above⁸. Using a mass-luminosity for our local volume of $(M/L)_B = 1.4$ (Flynn et al. 2006), we obtain a stellar mass column density of $\sim 0.57 \text{ } M_{\odot} \text{ pc}^{-2}$, again, 62 times smaller than the $35.5 \text{ } M_{\odot} \text{ pc}^{-2}$ in the local volume (see also Moni-Bidin et al. (2012)). Note that we do not correct these values for the effect of inclination on SB since our data suggest that Malin 1 is almost face-on.

As shown in all Figures we observe, for the first time, in full view, that Malin 1 is far from having a featureless low surface brightness disk. It presents rich features suggesting stellar formation regions and well defined spiral arms. We emphasize that these are well developed structures,

with an extremely low SB, which translates to extremely diffuse stellar density (as shown above). The data then suggests that morphological structures as observed here, can be long lived in this kind of LSBGs, and could imply large concentrations of dark matter (Seigar et al. 2014). The formation of spiral arms observed to such low stellar densities is another issue. This could be explained by the action of density waves in the matter distribution. However, such a theory is still in discussion by some authors (Choi et al. 2015). Or perhaps a better explanation for the spiral structure of Malin 1 is tidal driving or even shear driving (Dwarkadas & Balbus 1996), more consistent with the presumed past encounter between Malin 1 and the galaxy SDSSJ123708.91 + 142253.2, shown in the images of Figure 1 by the upper left arrow.

3.2. Streams and other features

We observe two diffuse and cigar-like features embedded in the disk of Malin 1, and seem to cross it radially. The shorter one labeled as A in Figure 3 is likely the disk of a galaxy with a bulge located at RA(J2000.0) 12:36:59 and DEC(J2000) +14:19:44. The SDSS database indicate that this object has a photometric redshift of 0.19 ± 0.05 , suggesting that this galaxy is in the background, i.e. about 30,000 km/s away from Malin 1. Its morphology, undisturbed by the presence of Malin 1 seems to confirm that its redshift estimate is correct. Nevertheless, this value should be confirmed spectroscopically in order to ensure this galaxy is not interacting with Malin 1. The other, larger structure, labeled as B in Figure 3 and also apparent in Figures 1 and 2, does not present any bulge and its nature is unclear. We do not discard that may be we are observing the jet of the active galactic nucleus of Malin 1, classified as a LINER from spectral data by Barth (2007), and as a high-excitation Seyfert galaxy by Impey & Bothun (1989). The other possibility, and perhaps the most likely, is that this feature is part of the claimed past interaction between Malin 1 and the galaxy SDSSJ123708.91 + 142253.2 approximately 1 Gyr ago, located at $\sim 350 \text{ kpc}$ from Malin 1 (Reshetnikov et al. 2010) (indicated by upper arrows in Figure 1). We note that this stream extends up to $\sim 200 \text{ kpc}$ from the center of Malin 1. We do not discard the relationship of these features with the presence of Malin 1B (see Figure 3), discussed in Reshetnikov et al. (2010).

3.3. Stellar formation regions?

The presence of several diffuse regions in the spiral arms exhibiting morphologies similar to stellar formation regions and/or clumps of gas is apparent. Examples of these clumps are labeled as R1, R2, R3, R4, R5 and R6 in Figure 3. Three of these regions (R1, R2 and R3) are the same as those observed by Braine et al. (2000) with the IRAM 30m telescope for detecting CO, unsuccessfully, though. These three regions were selected by Braine et al. (2000) after original observations by Bothun et al. (1987). This is the first time that such regions are so well defined in optical images.

3.4. Optical Diameter of Malin 1 and spiral arms thickness

One of the most impressive features of Malin 1 is its large diameter. Bothun et al. (1987, 1997) measured an

⁸ We have used $M_{\odot,B} = 5.45 \text{ mag}$ and a SB for the solar neighborhood of $27.02 \text{ mag arcsec}^{-2}$.

optical diameter of 110 kpc, almost 6.5 times larger than the diameter of the MW, making Malin 1 the largest disk/spiral galaxy in the universe so far. Considering a redshift of 0.082, a CCD pixel scale of 0.16 arcsec/pix, and the faintest spiral arm observed in the images shown in Figures 1 and 2, the optical diameter of Malin 1 turn to be about 160 kpc (750,000 light years). This is about 50 kpc (163,000 light years) larger than the diameter described by former authors (Pickering et al. 1997; Barth 2007). The double arrow in Figure 2 indicate a physical scale of 30.6 kpc, basically the size of the MW. Images show that Malin 1 is not only large, but also its spiral arms are scaled to gigantic proportions. Some sections in spiral arms of Malin 1 in Figure 2 measure $\sim 5 - 10$ kpc thick, i.e. approximately one third of the MW diameter.

4. CONCLUSIONS

In this letter we have obtained deep optical images of Malin 1, the faintest and largest giant LSBG so far, to unprecedented depth. The galaxy is composed by an inner bright region, well differentiated from the outer part composed by spiral arms. The color difference between the inner part and the spiral arms also appear extreme, with the former much redder than the spiral arms. We clearly see spiral arms and other structures down to a SB $\sim 28 B$ mag arcsec $^{-2}$. Comparing the resulting luminosity and stellar surface density of Malin 1 spiral arms with that derived for the disk of our Galaxy, we obtain $\sim 0.41 L_{\odot}$ pc $^{-2}$ and $\sim 0.57 M_{\odot}$ pc $^{-2}$, i.e. 62 times lower than those MW corresponding values. And yet, the galaxy exhibits a textbook and gigantic spiral structure, to these very low

density values. This is certainly the most astonishing result of this work. How spiral arms can form and remain long-lived to these very low density contrast, is beyond the scope of this letter. The deep g and r images reveal details for other features marginally observed in the past. In particular, we observe two conspicuous features with cigar-like morphology, crossing the spiral arms: one is very likely a background galaxy, and the other is a larger, faintest structure pointing to the galaxy SDSSJ123708.91 + 142253.2, claimed by Reshetnikov et al. (2010) to had interacted 1 Gyr ago with Malin 1. Our imaging does not allow to conclude about the nature of this structure. Other observed features seem to be stellar formation regions or gas clumps, some of them already observed by Braine et al. (2000) with the IRAM 30m telescope in order to detect CO, unsuccessfully, however. Our data also confirm that Malin 1 is even larger than previously reported, reaching 160 kpc diameter, i.e. more than 6.5 times the diameter of the MW. The fundamental result is that Malin 1 appears, at last, in full view in optical bands, allowing to see features that were not revealed before to such a detail and contrast.

GG, VS and LI acknowledge the support of Fondcyt regular 1120195 and Basal PFB-06 CATA. We are grateful to the Las Campanas Observatory staff. We appreciate discussions with Hugo Messias, Andrés Jordán, René Méndez and Márcio Catelan. We are grateful to the anonymous referee who helped to improve this letter.

REFERENCES

- Barth, A. 2007, *AJ*, 133, 1085
 Bothun, G., Impey, C., McGaugh, S. 1997, *PASP*, 109, 745
 Bothun, G., Impey, C., Malin, D., Mould, J. 1987, *AJ*, 94, 23
 Braine, J., Herpin, F., Radford, S. 2000, *A&A*, 358, 494
 Bredies, K., Kunisch, K., & Pock, T. 2010, *Total Generalized Variation*, *SIAM Journal on Imaging Sciences*, 2010, 3, (3), 492-526
 Choi et al. 2010, *ApJ*, 810, 9
 Conejero, J., Milovic, C., & Peris, V. 2015, *PixInsight Core 1.8.2*, Pleiades Astrophoto S.L., Spain. <http://www.pixinsigh>
 Dalcanton, J., Spergel, D., Gunn, J., Schmidt, M., Schneider, D. 1997, *AJ*, 114, 635
 Das, M., O’Neil, K., Vogel, S., McGaugh, S. 2006, *ApJ*, 651, 853
 Disney, M. 1976, *Nature*, 263, 573
 Dworkadas, V., Balbus, S. 1996, *ApJ*, 467, 87
 Flynn, Holmberg, J., Portinari, L., Burkhard, F., Jahreiß, H. 2006, *MNRAS*, 372, 1149
 Galaz, G., Herrera-Camus, R., Garcia-Lambas, D., Padilla, N. 2011, *ApJ*, 728, 74
 Galaz, G., Dalcanton, J., Infante, L., Treister, E. 2002, *AJ*, 124, 1360
 Impey, C., Sprayberry, D., Irwin, M., & Bothun, G. 1996, *ApJS*, 105, 209
 Impey, C., & Bothun, G. 1989, *ApJ*, 341, 89
 Jordi, K., Grebel, E. K., Ammon, K. 2006, *A&A*, 460, 339
 Koda, J., Yagi, M., Yamanoi, H., Komiyama, Y. 2015, [arXiv1506.01712](https://arxiv.org/abs/1506.01712)
 Krumholz, M., McKee, C. 2005, *ApJ*, 630, 250
 Lelli, F., Fraternali, F., Sancisi, S. 2010, *A&A*, 516, 11
 McGee, S., Balogh, M. 2010, *MNRAS*, 405, 2069
 Moni Bidin, C., Carraro, G., Mendez, R. A., Smith, R. 2012, *ApJ*, 751, 30
 Moore, L., Parker, Q. 2006, *PASA*, 23, 165
 Moore, B., Lake, G., Quinn T., Stadel, J. 1999, *MNRAS*, 304, 465
 O’Neil, K., Bothun, G., Impey, C. 2000, *ApJS*, 128, 99
 Pickering, T., Impey, C., van Gorkom, J., Bothun, G. 1997, *AJ*, 114, 1858
 Rahman, N., Howell, J., Helou, G., Mazzarella, J., Buckalew, B. 2007, *ApJ*, 663, 908
 Reshetnikov, V., Moiseev, A., Sotnikova, N. 2010, *MNRAS*, 406, 90
 Schlick, C., 1994. Quantization techniques for visualization of high dynamic range picture, *Photorealistic Rendering Techniques*, Springer-Verlag, P. Shirley, G. Sakas and S. Muller, Eds., 1994, 7-20.
 Seigar, Marc S., Davis, Benjamin L., Berrier, Joel, Kennefick, Daniel 2014, *ApJ*, 795, 90
 Seigar, M. 2008, *PASP*, 120, 945
 Sprayberry, D., Impey, C., Bothun, G., Irwin, M. 1995, *AJ*, 109, 558
 Stark, J. L., Murtagh, F. & Fadili, J., 2010. *Sparse Image and Signal Processing: Wavelets, Curvelets, Morphological Diversity*, Cambridge University Press, Cambridge (GB).
 Toomre, A., Toomre, J. 1972, *ApJ*, 178, 623
 van Dokkum, P., Romanowsky, A., Abraham, R., Brodie, J., Conroy, C., Geha, M., Merritt, A., Villaume, A., Zhang, J. 2015, *ApJ*, 804, L26

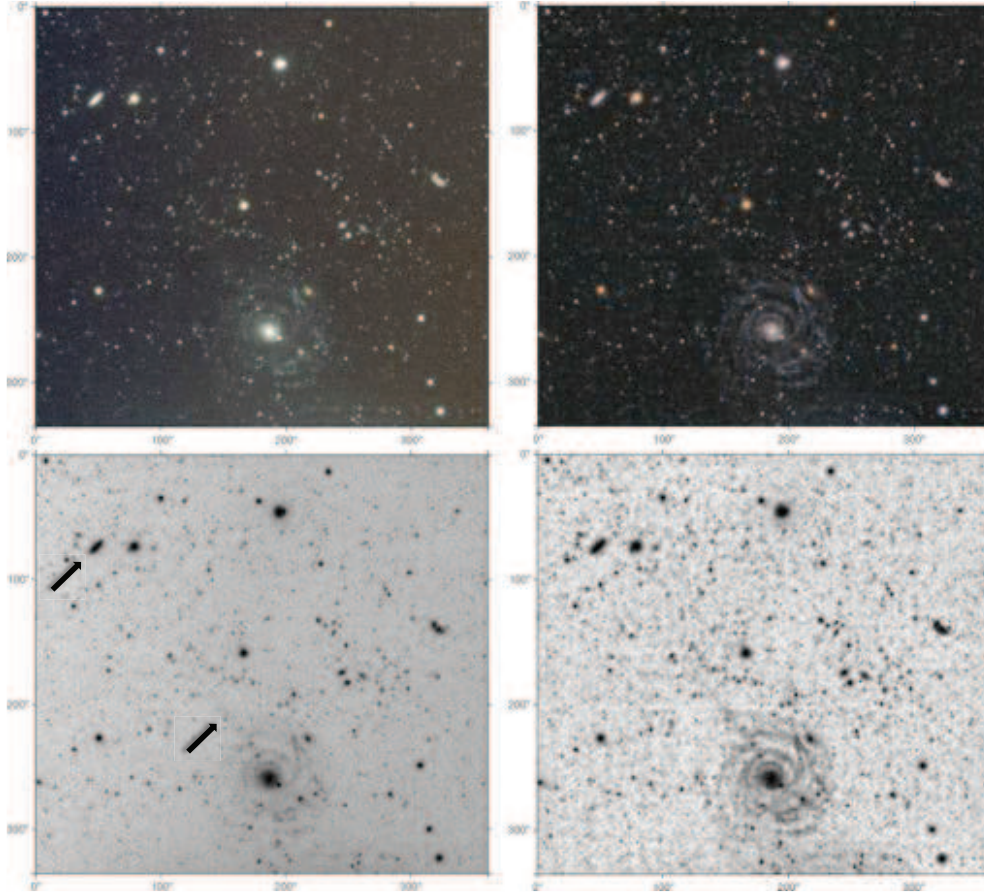


FIG. 1.— Processed images of Malin 1. Left panels: top panel, RGB image generated using the stacked and combined g and r images, totalizing about 4.5 hrs exposure time. Bottom, the same as the upper panel but a monochrome and inverted version of the same image. Right panels: the same as the left panels, but after applying the total generalized variation regularizator (TGV), and starlet transform for noise reduction and multi-scale processing. The enhancement of the spiral arms and other features discussed in the text are apparent after the TGV processing, comparing left and right panels. The upper left arrow indicate the galaxy SDSSJ123708.91 + 142253.2, which is claimed to had interacted 1 Gyr ago with Malin 1 (Reshetnikov et al. 2010). The near center arrow points a feature discussed in the text. The data used to create this figure is available [here](#).

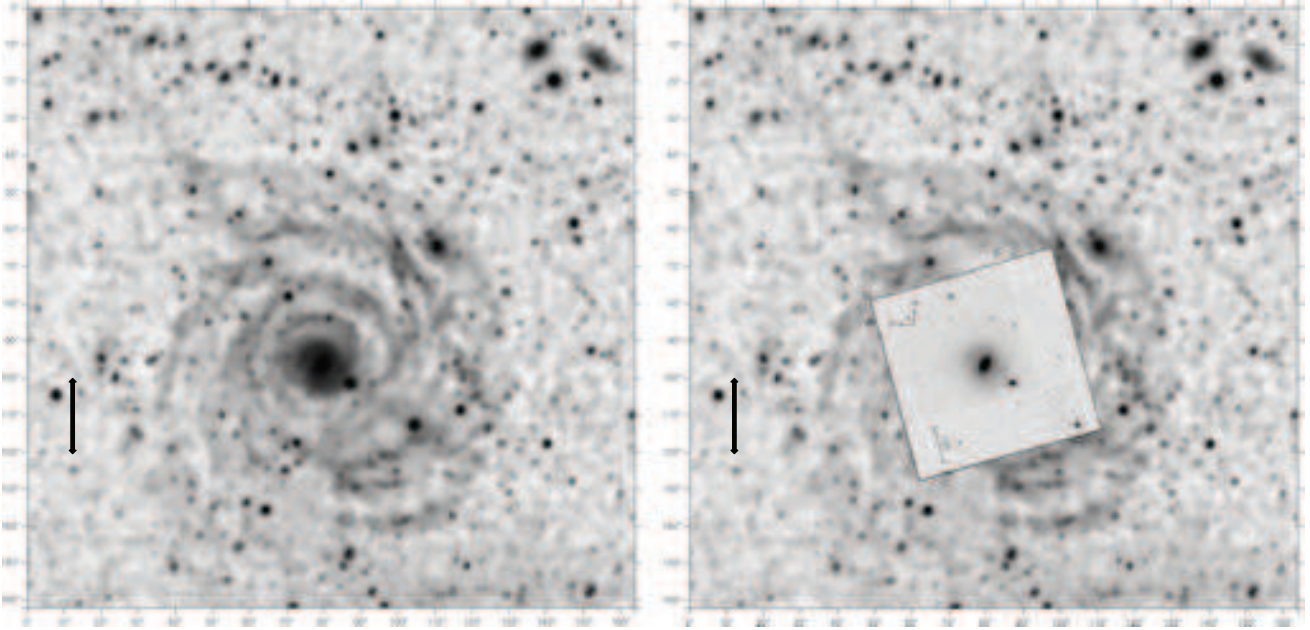


FIG. 2.— Zoom images of the monochrome versions of bottom right panel of Figure 1. In the right panel, an inset with an HST/WFPC2 image, from Barth (2007), is shown. Both panels include the image scale in arcsecs. The double arrows represent the physical scale (30.6 kpc, the approximate diameter of the Milky Way).

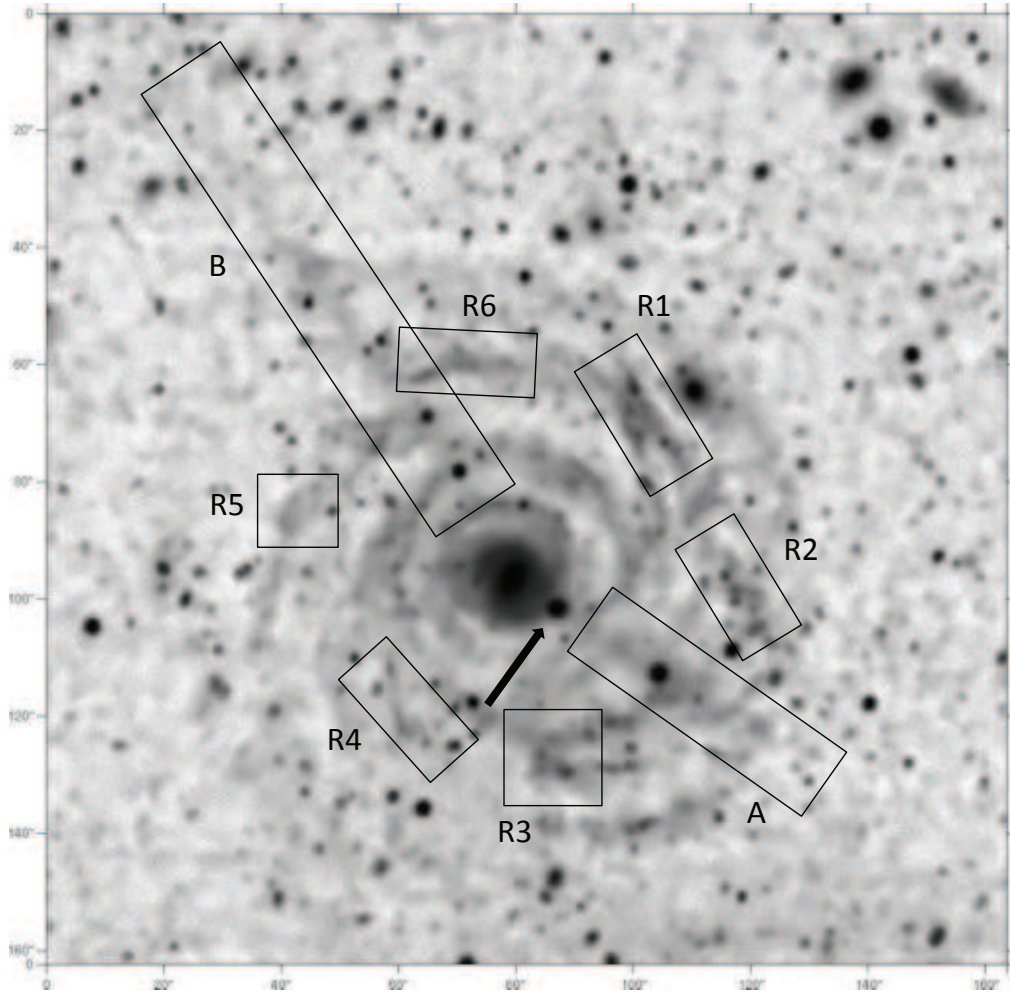


FIG. 3.— The same as left panel of Figure 2 but showing some regions discussed in the text. The arrow indicate the position of Malin 1B (Reshetnikov et al. 2010).